



## A Multi-Stage Clustering Approach for Cerebrospinal Fluid Image Segmentation

Afnizanfaizal Abdullah<sup>1,2\*</sup>, Akihiro Hirayama<sup>3</sup>, Satoshi Yatsushiro<sup>4</sup>, Mitsunori Matsumae<sup>3</sup>, Kagayaki Kuroda<sup>2,4</sup>

<sup>1</sup> Artificial Intelligence and Bioinformatics Group (AIBIG), Faculty of Computer Science and Information Systems, Universiti Teknologi Malaysia, 81310 UTM, Johor, Malaysia

<sup>2</sup> Course of Information Science and Technology, Graduate School of General Science and Technology, Tokai University, 4-1-1 Kitakaname, Hiratsuka, 259-1292, Japan

<sup>3</sup> Department of Neurosurgery, School of Medicine, Tokai University, Isehara, Kanagawa, 259-1188, Japan

<sup>4</sup> Department of Human and Information Sciences, School of Information Science and Technology, Tokai University, 4-1-1 Kitakaname, Hiratsuka, 259-1292, Japan

[afnizanfaizal@utm.my](mailto:afnizanfaizal@utm.my)

**Abstract:** Analysis of the cerebrospinal fluid (CSF) flow within brain has become increasingly important to diagnose a number of neurodegenerative disorders. Magnetic resonance imaging (MRI) is utilised to measure the CSF volumetric change in patients. However, the quality of the images is often hampered by partial volume effect, which blurred the boundary between the brain tissues and the CSF. Consequently, the accuracy of CSF analysis is reduced significantly. In this paper, we introduce a new multi-stage clustering approach to overcome this limitation. Firstly, the T1-weighted images are fused with the corresponding T2-weighted images. Next, the resulting images are subjected to partial volume estimation using Gaussian mixture model. The model produced by these images is later used as input in a spatial fuzzy clustering algorithm to segment the CSF flow from the brain tissues. Benchmark images obtained from BrainWeb are used to validate the performance of the proposed approach. In addition, we also presented the performance of the proposed method using real MRI images taken from a number of Alzheimer's disease patients, which evidently showed the effectiveness of the method in quantifying the CSF flow within the brain.

[Abdullah A., Hirayama A., Yatsushiro S., Matsumae M., and Kuroda K. **A Multi-Stage Clustering Approach for Cerebrospinal Fluid Image Segmentation.** *Life Sci J* 2020;17(12):59-66]. ISSN: 1097-8135 (Print) / ISSN: 2372-613X (Online). <http://www.lifesciencesite.com>. 8. doi:[10.7537/marlsj171220.08](https://doi.org/10.7537/marlsj171220.08).

**Keywords:** Image segmentation; image fusion, Gaussian mixture model; spatial Fuzzy C-Means

### 1. Introduction

Significance changes in normal cerebrospinal fluid (CSF) flow has been widely investigated, which showed its close connection to a number of neurodegenerative disorders, such as tumour, hydrocephalus and dementia. The CSF is a type of clear, colourless fluid that circulates within brain and spinal cord. The fluid plays important roles in conserving nutrients for the central nervous system (CNS), stabilizing certain chemical regulation within brain, as well as to avoid minor external damages caused by traumatic accidents. The CSF pulsatile movement can be used to detect disorders that caused small but substantial changes to the normal CSF volumetric measurements (Guoa et al., 2013). In other word, analysing CSF volumetric changes can be an effective diagnosis for critical disorders within human brain.

One of the biomedical imaging modalities is magnetic resonance imaging (MRI). This modality is capable to produce high resolution images among

different soft tissues. This is due to the fact that the MRI technique uses resonance of water molecules to generate signal that can be project into images. Thus, the MRI is commonly used to identify CSF flow within brain. The generated MRI images are facilitated by image processing techniques to approximate the CSF flow over the structure fragments, including brain tissues, more accurately. In most cases, image segmentation methods are implemented to distinguish different regions of the brain tissues, namely white matter (WM) and grey matter (GM), with CSF. The image segmentation methods can be characterised into three main categories: thresholding, region growing, and clustering methods. In thresholding methods, the images are segmented based on the intensity value of each voxel. Hence, the methods applied straightforward technique, in which the images are differentiate solely based on a certain threshold level of intensity. As a result, the methods are often vulnerable to image noise (Wu et al., 2007; Ahmed,

2010; Khan et al., 2013). On the other hand, the region growing methods are utilised statistical and derivative-based techniques to detect edges of a certain region in the images. Based on the information, the methods expanded the edges to the neighbouring voxels. However, these methods frequently required widespread prior knowledge, particularly in tuning operational parameters to enhance the segmentation accuracy (Forouzanfar et al., 2010).

In contrast to thresholding and region growing methods, the clustering methods seem to show more promising outcomes in terms of robustness. The methods are developed based on an unsupervised classification technique to collect image voxels into several groups with similar characteristics. The methods basically permit only small number of operational parameter adjustments. In particular, some of these methods exploit fuzzy-based adaptation to acclimate these parameters over different types of data sets (Benaichouche et al., 2013). Nevertheless, these methods usually required larger amount of computation time to perform better (Caldairou et al., 2009; Ji et al., 2010; İcer, 2013; Wang et al., 2013).

One of the challenging tasks in segmenting the CSF from the MRI brain images is partial volume effect (Aplerin et al., 2006). The partial volume effect is an image artefact that caused by the lack of the intensity between boundaries of certain regions in the images. Consequently, the CSF images are sometimes difficult to differentiate with the brain tissues. Few previous studies have considered incorporating spatial information from locally obtained voxels. For this case, level set theory has been employed to enhance the fuzzy clustering methods (Sundareswaran et al., 2009; Wang et al., 2011; Li et al., 2011b). Besides an outstanding capability of handling the partial volume effect, the methods also were able to segment images with minor adjustment of operational tunings (Zhang et al., 2004; Zhao et al., 2011; Li et al., 2011a). However, despite of the advantages, only a small number of previous works has been presented for identifying CSF flow within brain, particularly to detect CSF segmentation to quantify the changes of normal volumetric information.

Recently, a number of researches has currently focused on image fusion techniques to enhance the information of the images (Landman et al., 2012). Image fusion is used to combine visual data from different types of images that might include imperative information of a specific region of the image (Tian et al., 2013; Xu, 2013). Yang and Li (2012) presented a new image fusion technique based on local pixel level using simultaneous orthogonal matching scheme. This technique is aimed to exploit local information of the images by overlapping the

image patches based on signal sparse representation. The utilization of local information in the images is crucial for image fusion techniques. Therefore, Shen et al. (2013) proposed an improved cross-scale coefficient selection rule to improve the consistency of image fusion technique. This improvement particularly utilized the neighbouring information of the image pixels in a different set of same images. Hence, local information is highly exploited to quantify abnormalities in the images that may represent specific diseases in patients. On contrary, Xu (2013) has designed a new image fusion technique that utilized multiple levels of the local information. In this contribution, selection rule is implemented in distinguishable layers, preserving information of the source images while enhancing the quality of the fused images.

In this paper, we introduce a new multi-stage clustering method for segmenting CSF flow within human brain, with a consideration of handling partial volume effect. The proposed method comprised three major stages, namely image fusion, boundary detection, and spatial fuzzy segmentation. In the first stage, the collected T1- and T2-weighted MRI images are fused. Later, Gaussian mixture modelling was employed to detect boundaries within the fused images. This is an important stage, which the boundary between the CSF and brain tissues, namely WM and GM, is statistically differentiated locally. This stage generated a mathematical model that provides information of the boundary intensity, giving a threshold between the blurring voxels. For the spatial fuzzy segmentation stage, the original MRI images were segmented based on the model produced by the previous stage. A set of MRI images was collected from BrainWeb repository (Cocosco et al., 1997). In addition, real MRI images of 15 Alzheimer's disease patients were also obtained from Alzheimer's Disease Neuroimaging Initiative (ADNI) database (Jack et al., 2008) for the validation. The experimental results showed that the proposed method was capable to detect CSF flow significantly, while simultaneously, handling the problem of partial volume effect more effectively compare to the existing methods.

## 2. Proposed Multi-Stage Clustering Approach

In this paper, a new multi-stage clustering method is proposed for CSF segmentation in the MRI images while handling the partial volume effect. The proposed method is consisted of three stages: image fusion, boundary detection, and spatial fuzzy segmentation stages. The detail of the proposed method is presented in the following sections.

### 2.1 Image Fusion Stage

The proposed method employed a straightforward image fusion stage, in which no prior image registration is implemented. Instead, the images to be combined are assumed to be perfectly registered, in a sense that each voxel in the two images is matched. Let say  $I_a$  and  $I_b$  are two images, namely

T1- and T2-weighted MRI images respectively. The images are mapped together, in a sense that obvious characteristics, such as object boundaries, are fit perfectly. To ensure this, each input images are decomposed into subunit quadrants. Figure 1 illustrates the mapping and fusion procedure.

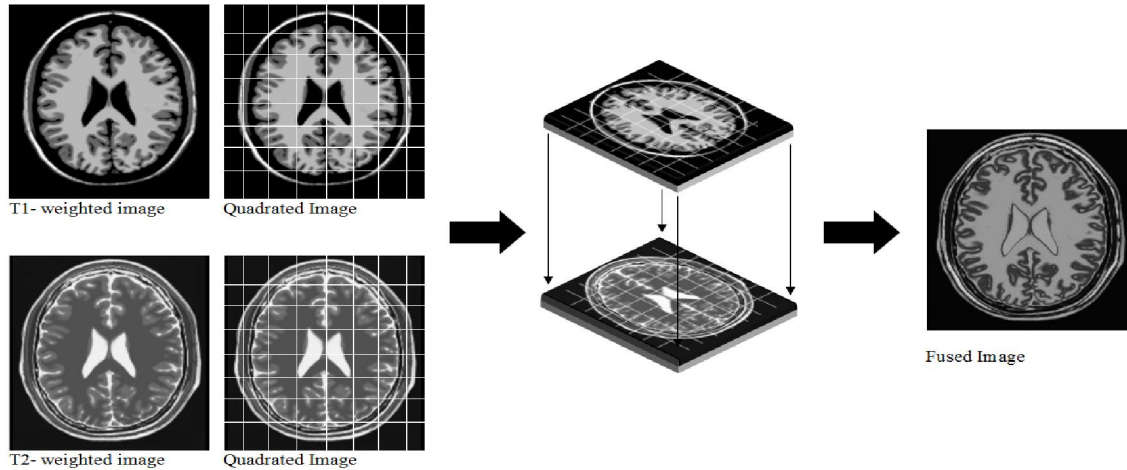


Figure 1. Image mapping and fusion

### 2.2 Boundary Detection Stage

The expectation-maximization (EM) method is often used to estimate the parameters in the mixture modelling approach. The method is generally developed based on the iterative technique, which aims to optimize the likelihood function when some information is absent. In the context of image segmentation, this missing information is usually formulated as the class membership of the intensity values in the images. Accordingly, let  $x_i$  be the intensity value of the  $i$ th pixel in the image  $I$ . In general, given  $C$  number of classes, the intensity value  $x_i$  may belong to one of the classes with different probabilities,  $g(x_i)$ . Thus, the probability of the intensity value  $x_i$  may belong the class as given as the following equation:

$$g(X | p) = \sum_{j=1}^C w_j g_j(x_i | p_j)$$

where  $w_j$  is the weighting coefficient of the  $j$ th cluster,  $X = \{x_1, x_2, x_3, \dots, x_D\}$  is the  $D$ -dimensional data vector (image) and  $p_j = \{\mu_j, \dot{\Sigma}_j\}$  is a parameter set consists of two vectors, mean  $\mu$  and covariance matrix  $\dot{\Sigma}_j$ , given by the following equations:

$$\mu_{j(t+1)} = \frac{1}{N} \sum_{i=1}^N \frac{g(p_j | x_i) x_i}{w_{j(t+1)}}$$

$$\dot{\Sigma}_{j(t+1)} = \frac{1}{N} \sum_{i=1}^N \frac{g(p_j | x_i) (x_i - \mu_{j(t+1)}) (x_i - \mu_{j(t+1)})^T}{w_{j(t+1)}}$$

where  $N$  is the total number of voxels in the image. In most cases, the distributions of the probabilities for intensity values are illustrated using histogram, in which the modes may represent the classes or clusters of the images. Based on this equation, the parameter set is commonly unknown and often estimated using the iterative optimization method, namely EM method.

The EM method is consisted of two major steps: expectation (E-step) and maximization (M-step) steps. At each iteration, these steps are executed interchangeably until the value of the following equation is locally stagnant

$$\log g(X | p) = \log \prod_{n=1}^N g(x_n | p)$$

In the E-step, the log likelihood of a complete image is constructed as following the equation:

$$\log g(X | p) = \sum_{n=1}^N \sum_{j=1}^C e_j^n \log [w_j g(x_n | p_j)]$$

where

$$\varepsilon_j^n = g(j | x_n, p_{(t)}) = \frac{w_j g(x_n | p_{j(t)})}{\sum_{k=1}^c w_k g(x_n | p_{k(t)})}$$

is the posterior probability and  $p_{(t)}$  is the parameter estimated at  $t$  iteration (Pernkopf and Bouchaffra, 2005; Li et al., 2013; İçer, 2013). Alternatively, the M-step performs the estimation of  $p_{(t+1)}$  according to the value of  $\varepsilon_j^n$ , in which the parameters  $w_{j(t+1)}$ ,  $\mu_{j(t+1)}$ , and  $\dot{\Sigma}_{j(t+1)}$  are revised accordingly as follows:

$$w_{j(t+1)} = \frac{1}{N} \sum_{n=1}^N \varepsilon_j^n$$

$$\mu_{j(t+1)} = \frac{\sum_{n=1}^N \varepsilon_j^n x_n}{\sum_{n=1}^N \varepsilon_j^n}$$

$$\dot{\Sigma}_{j(t+1)} = \frac{\sum_{n=1}^N \varepsilon_j^n (x_n - \mu_{j(t+1)})(x_n - \mu_{j(t+1)})^T}{\sum_{n=1}^N \varepsilon_j^n}$$

Based on this estimation, the boundary of CSF can be differentiated from the brain tissue more effectively. This is due to the fact that the image intensity provided by the each voxel is represented in the form of histogram, which the thresholds are determined repeatedly by the method. Figure 2 illustrates the boundary detection in this stage.

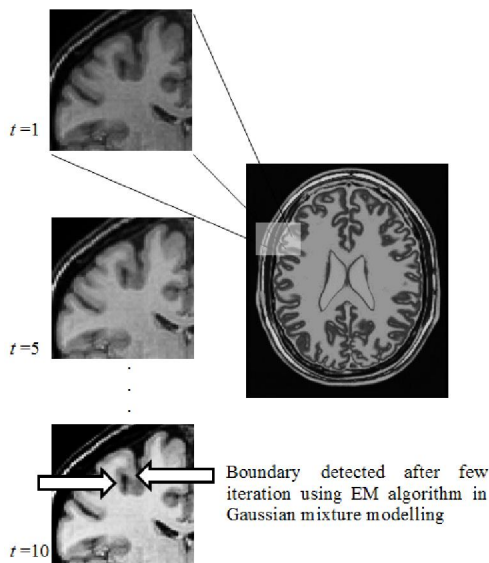


Figure 2. Boundary detection stage

### 2.3 Spatial Fuzzy Segmentation Stage

The fuzzy c-means (FCM) method has been regularly utilised for image segmentation. The method is fundamentally used to cluster distinctive regions within an image according to fuzzy-based membership values assigned to each voxel. However, only a small number of contributions have been done that focused on the CSF segmentation. Compare to hard clustering methods, for instance k-means clustering method, the membership assigned to each voxel allowed the FCM method to congregate the voxel into different groups. In other word, the voxels could be belonged to more than one group, depending on the characteristics shared by the different groups. More recently, an increasingly number of researches has penetrated spatial information of the neighbouring voxels during the clustering process. Instead of having only a single voxel to be evaluated, the spatial information considered the values collected from the surrounding area of each voxel, which being incorporated to the membership value of the current voxel. Given an image,  $I$ , which contained a set of voxels. Each  $i$ th voxel is assigned with a corresponding intensity value,  $x_i$ . Assume that this image is subjected for a segmentation process, where each voxel would be grouped into  $C$  clusters. Hence, each  $i$ th voxel,  $x_i$ , is assigned with a fuzzy membership value given by the following set:

$$u_{ij}^C = \{u_{i1}, u_{i2}, u_{i3}, \dots, u_{iC}\}$$

where each voxel is grouped into each cluster by the following rule

$$\sum_{j=1}^C u_{ij} = 1$$

in which  $u_{ij} \in [0,1]$  and for all  $j$ ,  $j \in [1, C]$ . A

cluster centroid,  $y_j$ , is assigned for each  $j$ th cluster. The cluster centroid is generally used to represent the mean intensity value of the voxels in the given cluster (Caldairou et al., 2009). By using this information, an objective function is defined as follows

$$f(u, y_j) = \arg \min \sum_{i=1}^N \sum_{j=1}^C u_{ij}^\alpha \|x_i - y_j\|$$

where  $N$  is the total number of voxels, and  $\alpha$  is a control parameter, in such a way that the value of  $\alpha$  must be more than 1. The spatial FCM method would be repeatedly update the membership values and the cluster centroid based on the following equations:

$$u_{ij} = \frac{u_{ij}^\alpha h_{ij}^\beta}{\sum_{k=1}^C u_{kj}^\alpha h_{kj}^\beta}, \quad h_{ij} = \sum_{k \in w(x_i)} u_{ik}$$

$$y_j = \frac{\sum_{i=1}^N u_{ij}^\alpha y_j}{\sum_{i=1}^N u_{ij}^\alpha}$$

where  $h_{ij}$  is the spatial value,  $w(x_i)$  is a square window centred by the current  $i$ th voxel, and  $\beta$  is another control parameter (Li et al., 2011a; Chuang et al., 2006). Thus, the spatial value  $h_{ij}$  is comparatively huge when most of the neighbouring voxels are belonged to the same cluster. This also helps the method to avoid voxels that supposedly not belong to the cluster, giving a capability to handle measurement noise more effectively (Chuang et al., 2006).



Figure 3. Example of image segmentation up to 550 iterations

### 3. Experimental Results

In this paper, the effectiveness of the proposed method in terms of segmenting the CSF flow with the presence of partial volume effect was evaluated using MRI images obtained from BrainWeb repository. These images were produced by simulation using a set of MRI data volume information given by the users. A number of 20 images were generated based on the following parameters: repetition time (TR) of 22ms; echo time (TE) of 9.2ms; flip angle of 30 degree; and isotropic voxel size of 1mm. The manual segmentation of these images was taken as the ground truth to compare the accuracy performance of the automatic segmentation by the proposed method over the existing methods, namely standard EM, FCM, and spatial FCM. Table 1 to 4 present the accuracy of the segmentation produced by the proposed method compared to other methods for MRI images with 3%, 5%, 7%, and 9% measurement noise added, respectively. The similarity index,  $S_{index}$ , is calculated as follows

$$S_{index} = \frac{I_{gnd} \cap I_{seg}}{I_{gnd} + I_{seg}}$$

where  $I_{gnd}$  and  $I_{seg}$  are the ground truth and segmentation produced by the methods, respectively. Each method was subjected for 100 independent runs, in which the average of the similarity index and the corresponding standard deviation were calculated. This is to ensure that the results were recorded with fair justification. According to the results presented in Table 1 to 4, the accuracy of the segmentation by the proposed method has outperformed the existing counterparts. For the CSF segmentation, in particular, the segmented images by the proposed method have showed significantly better compared to the other methods. This is crucial due to the fact that the method needed to perform well in this region of interest, permitting better analysis of the CSF volumetric changes provided by the images.

Table 1. Average similarity index for 20 MRI images (with 3% noise)

Region	Average Similarity Index, $S_{index}$			
	EM	FCM	SFCM	Proposed
WM	0.85±0.07	0.88±0.05	0.90±0.06	0.97±0.02
GM	0.79±0.10	0.80±0.09	0.85±0.09	0.90±0.05
CSF	0.82±0.05	0.85±0.02	0.89±0.04	0.95±0.03

Table 2. Average similarity index for 20 MRI images (with 5% noise)

Region	Average Similarity Index, $S_{index}$			
	EM	FCM	SFCM	Proposed
WM	0.80±0.08	0.83±0.06	0.85±0.05	0.95±0.03
GM	0.72±0.09	0.74±0.10	0.77±0.08	0.89±0.07
CSF	0.78±0.03	0.80±0.05	0.82±0.07	0.92±0.05

Table 3. Average similarity index for 20 MRI images (with 7% noise)

Region	Average Similarity Index, $S_{index}$			
	EM	FCM	SFCM	Proposed
WM	0.78±0.06	0.80±0.06	0.83±0.08	0.89±0.05
GM	0.69±0.12	0.73±0.09	0.75±0.10	0.82±0.08
CSF	0.75±0.05	0.78±0.08	0.80±0.05	0.84±0.05

Table 4. Average similarity index for 20 MRI images (with 9% noise)

Region	Average Similarity Index, $S_{index}$			
	EM	FCM	SFCM	Proposed
WM	0.73±0.07	0.78±0.05	0.80±0.07	0.85±0.04
GM	0.65±0.10	0.67±0.09	0.71±0.11	0.77±0.09
CSF	0.69±0.06	0.73±0.05	0.79±0.05	0.82±0.08

The proposed method was also evaluated using real Alzheimer's disease patient MRI brain images. The images were obtained from ADNI database. In this experiment, 15 patients are selected. The images were taken from patients with an average age of  $84.85 \pm 7.75$  years old. The images were acquired using 3.0T Philips Medical Systems based on the following setup: flip angle=15.0 degree, slice thickness=10.0mm, TE=4.60ms, TR=11.12ms. Table 5 presents the average similarity index produced by

the proposed method compared to the existing EM, FCM, and SFCM methods. The ground truths of these images were generated by the manual segmentation performed by experts. Despite of the presence of partial volume effect, the proposed method has shown potential capability in sustaining the robustness of the segmentation accuracy. Figure 4 illustrates the example of the CSF segmentation produced by the proposed method.

Table 5. Average similarity index for 15 Alzheimer's disease patient MRI images

Region	Average Similarity Index, $S_{index}$			
	EM	FCM	SFCM	Proposed
WM	0.59±0.12	0.65±0.08	0.71±0.06	0.78±0.06
GM	0.45±0.23	0.57±0.19	0.65±0.10	0.70±0.07
CSF	0.53±0.09	0.60±0.05	0.75±0.06	0.75±0.02



Figure 4. A series of segmented CSF images showed the CSF flow within brain tissues

#### 4. Conclusion

In this paper, we introduced a new multi-stage clustering approach for segmenting CSF flow within

MRI brain images. In principle, the proposed consisted of three stages, namely image fusion, boundary detection, and spatial fuzzy clustering

stages. The proposed method firstly combined two different images of different weighted schemes into a single image. This stage is important because the combined image might contained more information, as the different weighted images consisted of distinctive characteristics. Next, the proposed method identified the boundary of CSF region using Gaussian mixture modelling. This stage is executed to obtain information of the CSF layer and played as a primary step to handle partial volume effect as different boundaries in the image were substantially distinguished. Lastly, the method performed image segmentation using spatial fuzzy clustering based on the information given in the previous stage. The method has been verified using both simulated and clinically obtained MRI images. The experimental results showed that the segmentation accuracy of the proposed method has outperformed existing method effectively. This provides a new direction of identifying neurodegenerative diseases by segmenting CSF flow within human brain.

#### Acknowledgment

We would like to express our gratitude to Universiti Teknologi Malaysia (UTM), and Tokai University, Hiratsuka, Japan, for providing funding and facility supports for this project.

#### Corresponding Author:

Dr. Afnizanfaizal Abdullah  
Artificial Intelligence and Bioinformatics Group (AIBIG), Faculty of Computer Science and Information Systems, Universiti Teknologi Malaysia, 81310 UTM, Johor, Malaysia  
E-mail: [afnizanfaizal@utm.my](mailto:afnizanfaizal@utm.my)

#### References

- Ahmed M.M. (2010), A parametric model for the segmentation of brain magnetic resonance images, PhD. Thesis, Universiti Teknologi Malaysia.
- Alperin N., Mazda M., Lichtor T. and Lee S.H. (2006), From cerebrospinal fluid pulsation to noninvasive intracranial compliance and pressure measured by MRI flow studies, *Current Medical Imaging Reviews*, 2(1), 117-129.
- Benaichouche A. N., Oulhadj H., and Siarry P. (2013), Improved spatial fuzzy c-means clustering for image segmentation using PSO initialization, Mahalanobis distance and post-segmentation correction, *Digital Signal Processing*, 23(5), 1390-1400.
- Caldairou B., Rousseau F., Passat N., Habas P., Studholme C. and Heinrich C. (2009), A non-local fuzzy segmentation method: Application to brain MRI, *Computer Analysis of Images and Patterns*, 44(9), 606-613.
- Chuang K.S., Tzeng H.L., Chen S., Wu J., Chen T.J. (2006), Fuzzy c-means clustering with spatial information for image segmentation, *Computation in Medical Imaging and Graphics*, 30(1), 9-15.
- Cocosco C. A., Kollokian V., Kwan R. K. S., Pike G. B., and Evans A. C. (1997), BrainWeb: Online interface to a 3D MRI simulated brain database, *NeuroImage*, 5, 425.
- Forouzanfar M., Forghani N. and Teshnehlab M. (2010), Parameter optimization of improved fuzzy c-means clustering algorithm for brain MR image segmentation, *Engineering Applications of Artificial Intelligence*, 23(2), 160-168.
- Guoa F., Lib Z., Songa L., and Liua X. (2013), One exceedingly rare co-existence of pituitary adenoma with hydrocephalus and cerebral aneurysm: case report and literature review, *Life Science Journal*, 10(2), 1719-1723.
- İçer S. (2013), Automatic segmentation of corpus collasum using Gaussian mixture modeling and Fuzzy C means methods, *Computer Methods and Programs in Biomedicine*, 112(1), 38-46.
- Jack C.R., Bernstein M.A., Fox N.C., Thompson P., Alexander G., Harvey D., Borowski B., Britson P.J., Whitwell J., Ward C. (2008), The Alzheimer's disease neuroimaging initiative (ADNI): MRI methods, *Jour. of Mag. Res. Ima*, 27(4), 685-691.
- Ji Z.X., Chen Q., Sun Q.S., Xia D.S. and Heng P.A. (2010), MR image segmentation and bias field estimation using coherent local and global intensity clustering, *Seventh International Conference on Fuzzy Systems and Knowledge Discovery (FSKD)*, 2, 578-582.
- Khan A. K., Raja G., and Khan A. K. (2013). Implementation of Marker based Watershed Image Segmentation on Magnetic Resonance Imaging. *Life Science Journal*, 10(2), 115-118.
- Landman B. A., Asman A. J., Scoggins A. G., Bogovic J. A., Xing F., and Prince J. L. (2012), Robust statistical fusion of image labels, *IEEE Transactions on Medical Imaging*, 31(2), 512-522.
- Li B.N., Chui C.K., Chang S. and Ong S.H. (2011a), Integrating spatial fuzzy clustering with level set methods for automated medical image segmentation, *Computers in Biology and Medicine*, 41, 1-10.
- Li C., Huang R., Ding Z., Gatenby J., Metaxas D. and Gore J. (2011b), A Level Set Method for Image Segmentation in the Presence of Intensity Inhomogeneities With Application to MRI, *IEEE*

- Transactions on Image Processing, 20(7), 2007-2017.
16. Li C., Wang X., Li J., Eberl S., Fulham M., Yin Y., and Feng D. D. (2013), Joint Probabilistic Model of Shape and Intensity for Multiple Abdominal Organ Segmentation From Volumetric CT Images, *IEEE Journal of Biomedical and Health Informatics*, 17(1), 92-102.
  17. Pernkopf F., and Bouchaffra D. (2005), Genetic-based EM algorithm for learning Gaussian mixture models. *IEEE Transactions on Pattern Analysis and Machine Intelligence*, 27(8), 1344-1348.
  18. Shen R., Cheng I., and Basu A. (2013). Cross-Scale Coefficient Selection for Volumetric Medical Image Fusion, *IEEE Transactions on Biomedical Engineering*, 60(4), 1069-1079.
  19. Sundareswaran K.S., Frakes D.H., Fogel M.A., Soerensen D.D., Oshinski J.N. and Yoganathan A.P. (2009), Optimum fuzzy filters for phase-contrast magnetic resonance imaging segmentation, *Journal of Magnetic Resonance Imaging*, 29(1), 155-165.
  20. Tian J., Wang Y., Dai X., and Zhang X. (2013), Medical image processing and analysis. In *Molecular Imaging* (pp. 415-469). Springer Berlin Heidelberg.
  21. Wang Z., Song Q., Soh Y. C., and Sim K. (2013), An adaptive spatial information-theoretic fuzzy clustering algorithm for image segmentation, *Computer Vision and Image Understanding*, 117(10), 1412-1420.
  22. Wang Y., Wang L., Xiang S. and Pan C. (2011), Level set evolution with locally linear classification for image segmentation, 18th IEEE International Conference on Image Processing (ICIP), 3361-3364.
  23. Wu J., Pian Z., and Guo L. (2007), Medical imaging thresholding algorithm based on fuzzy set theory, *The 2nd IEEE Conference on Industrial Electronics and Applications*, 919-924.
  24. Xu Z. (2013), Medical image fusion using multi-level local extrema, *Information Fusion*, <http://dx.doi.org/10.1016/j.inffus.2013.01.001>.
  25. Yang B., and Li S. (2012), Pixel-level image fusion with simultaneous orthogonal matching pursuit, *Information Fusion*, 13(1), 10-19.
  26. Zhang D.Q. and Chen S.C. (2004), Robust image segmentation using FCM with spatial constraints based on new kernel-induced distance measure, *IEEE Transactions on Systems, Man, and Cybernetics, Part B: Cybernetics*, 34(4), 1907-1916.
  27. Zhao S., Zhang D., Song X. and Tan W. (2011), Segmentation of hippocampus in MRI images based on the improved level set, *Fourth International Symposium on Computational Intelligence and Design (ISCID)*, 1, 123-126.

12/13/2020